Water dynamical anomalies evidenced by molecular-dynamics simulations at the solvent-protein interface

Claudia Rocchi, Anna Rita Bizzarri, and Salvatore Cannistraro*
Unitá INFM, Dipartimento di Fisica dell'Università, I-06100 Perugia, Italy
and Dipartimento di Scienze Ambientali, Università della Tuscia, I-01100 Viterbo, Italy
(Received 14 August 1997)

We present a computer simulation picture of the dynamical behavior, at room temperature, of water in the region close to a protein surface. We analyzed the probability distribution of water molecules diffusing near the surface, and we found that it deviates from a Gaussian, which is predicted for Brownian particles. Consistently, the mean square displacements of water oxygens show a sublinear trend with time. Moreover, the relaxation of hydration layers around the whole protein is found to follow a stretched exponential decay, typical of complex systems, which could as well be ascribed to the non-Gaussian shape of the propagator. In agreement with such findings, the analysis of water translational and reorientational diffusion showed that not only are the solvent molecule motions hindered in the region close to the protein surface, but also the very nature of the particle diffusive processes, both translational and rotational, is affected. The deviations from the bulk water properties, which put into evidence a deep influence exerted by the protein on the solvent molecule motion, are discussed in connection with the presence of spatial (protein surface roughness) and temporal (distribution of water residence times) disorder inherent in the system. [S1063-651X(98)07003-2]

PACS number(s): 87.15.−v, 66.10.−x

I. INTRODUCTION

It is currently generally agreed that proteins and their surrounding solvent environment exist in a sort of symbiosis [1–4]. Proteins are complex systems, exploring in their motion a huge amount of different conformational substrates (CS), thermally activated and related to local minima of the potential energy surface [5–8]. At room temperature, fluctuations among CS occur continuously, and are crucial in determining the macromolecule biological function [5]. The dynamical interaction of the protein-water system plays a very important role in the activation of these fluctuations. It has been suggested that the multiplicity of the surrounding water hydrogen bond (HB) patches, rearranging continuously, could be at the origin of the conformational motions of the biomolecule [3], the long flexible lateral chains being well suited to adapting to the many possible HB patterns [9]. This coupling suggests a close correlation between the solvent properties and the distribution of CS. In this context, it has been widely recognized that the biological functionality of a protein needs a minimum amount of water to be activated [4,10,11]. Moreover, a decrease in the hydration level leads in general to an inhibition of the protein mobility [4,11], in particular of those collective anharmonic motions which seem to be connected to CS transitions involving the rearrangement of a large number of atoms [12]. When the temperature is lowered, transitions among CS can be suppressed and the protein ends up being frozen in a kinetically arrested metastable state that is reminiscent of a glasslike system, which is characterized by short- (β) and long- (α) time scale relaxations [13,14]. The path to this so-called glass transition, which in proteins occurs at a T_g of about 220 K, has been found to be highly dependent on the solvent properties [13].

On the other hand, it was realized long ago that proteins influence both the spatial and the dynamical arrangement of their neighboring water layers [2,15,16]. A large deviation of the thermodynamic properties from those of bulk water was observed; for example, suppression of water freezing at low temperatures in the first hydration shell of myoglobin has been monitored by calorimetry [3,10,17]. Moreover, water mobility is significantly affected by the interaction with the protein surface. The dynamics of forming and rupturing of the solvent HBs with suitable protein atoms is found to be dependent on the chemicophysical properties of the amino acids belonging to the protein surface [16,18,19]. In particular, the analysis of the solvent molecule residence times, in local atomic hydration shells, has shown a larger permanence of water molecules in proximity to charged and polar residues, with respect to that found from simulations of bulk water [18,20,21]. Global water dynamical properties in shells around the protein are found to depend on the distance from the biomolecule surface [2,22–24]. In particular, the mean square displacements, evaluated by molecular dynamics (MD) simulations, of water molecules which move in the region close to the protein surface, are found to be sublinear with time [22,23,25]: this result is also confirmed by neutron scattering measurements [26]. Furthermore, when the water mean square displacement is decoupled into a parallel and a perpendicular component with respect to the protein surface, the anomalous sublinear trend, which is present in both the components, is found to be strongly anisotropic [23].

In this context, the study of the solvent-macromolecule interface region, which is characterized by the strongest coupling between the two entities, is of crucial importance in understanding the influence that protein and water exert on each other.

*Author to whom correspondence should be addressed. Electronic address: cannistraro@pg.infn.it

MD simulations, which up to now are able to study, with atomic resolution, a protein system in an explicit solvent environment up to a few nanoseconds, are particularly suited to investigating the water-protein interface.

The aim of this paper is to give a global picture of the water dynamical properties within hydration layers around the protein and try to reconcile all the anomalous features in the framework of models which describe the motion of particles in disordered systems [27,28].

In Sec. II we discuss in detail the MD methods employed to get the simulated trajectories. Section III is divided into two subsections where we present the results. The first deals with the probability distribution of water molecules and two related dynamical quantities: the water mean square displacements and the hydration shell relaxation functions. In the second, translational and reorientational velocity time-correlation functions are investigated. In Sec. IV a discussion of the previous results is reported, in connection with models describing random walkers in the presence of topological and temporal disorder inherent in the system [27,28]. Conclusions are drawn in Sec. V.

II. COMPUTATIONAL METHODS

The simulated trajectories of all the atoms of plastocyanin (PC), a copper-containing protein involved in photosynthetic electron transport, and of their surrounding water molecules, have been determined using the GROMOS program package [29] including the extended simple point charge (SPC/E) potential for water [30]. The initial coordinates have been obtained by the x-ray crystal structure at 1.33 Å resolution [31] (1 PLC entry from the Protein Data Bank). The PC x-ray structure consists of a single polypeptide chain containing 99 amino acids, a copper atom, and 110 crystallization waters. The copper atom is bonded to two side chain nitrogen atoms and two side chain sulfur atoms which form a distorted tetrahedral site with hydrophobic character [32]. To describe the copper-ligand interactions, a covalent bond was introduced for each ligand to preserve the x-ray structure [20,22], on the basis of spectroscopic evidences pointing out a strong covalent nature of these bonds [33]. The charge of the copper atom in such a model corresponds to $+0.6e$. With the exception of copper ligands, all the ionizable residues are assumed to be in their fully charged state, according to the value of $p\mathrm{H}=6$ as reported in the crystallographic work [31]. The protein molecule was centered in a truncated octahedral box obtained from a cube of edge 5.986 57 nm, and periodic boundary conditions were applied. The box was filled with 3103 water molecules, i.e., 5.32 g of water per g of protein. Cutoff radii of 0.8 nm for the nonbonded interactions and of 1.1 nm for the long-range charged interactions were used. Initial atomic velocities were assigned from a Maxwellian distribution corresponding to 300 K [34]. Any residual translational motion of the center of mass was removed from the initial velocities. The simulations were carried out in the canonical ensemble (nvt) [34]. The temperature of the system was held constant by weak coupling to an external bath of 300 K by using a temperature relaxation time of 0.01 ps for the first 10 ps and of 0.1 ps for the remaining simulation run. A decreasing positional restraining force, with a constant going from 9000 to 50 kJ/mol nm^2 was also applied during the first 20 ps. The Shake constraint algorithm [35] was used throughout the simulations to fix the internal geometry of the water molecules and to keep bond lengths of protein rigorously fixed at their equilibrium positions. The simulation extended over 600 ps, the first 100 of which were used for equilibration. The resulting root mean square deviation for all the protein atoms, from the x-ray structure, averaged over the last 500 ps, is 0.18 ± 0.02 nm. Trajectories and energies have been calculated with an integration step of 0.002 ps and collected every 0.1 ps. Other details of the simulation procedure are reported elsewhere [36]. A part of the simulation, from 200 to 210 ps, has been repeated storing trajectories every 0.002 ps to provide a data set accurate enough to study short-time dynamics.

III. RESULTS

In order to better put into evidence the influence exerted by the protein on its neighboring water layers, the dynamical quantities discussed in this section have been evaluated in water shells, around the whole protein, involving increasing distances from the macromolecule surface. Three water layers of different thickness R have been defined: the first includes superficial solvent molecules moving within 4 Å from the protein surface; the others concern waters which walk within larger distances ($R=6$ Å, $R=14$ Å), with the widest region including almost all the water molecules around the protein macromolecule investigated. Since water molecules can migrate from one shell to another during the simulation run, the check of the belonging of a water to a layer only at the beginning of the time interval investigated could lead to an incorrect evaluation of the averages and of time-correlation functions. Therefore we classified the belonging of each water molecule to a layer at each MD configuration step and we followed the water trajectory for subsequent times. Such a classification scheme, which we have already used in our previous work [20], was also in agreement with that employed in Refs. [21, 37].

A. Probability distribution

In the MD description, the solvent fluid can be considered as a statistical ensemble of particles whose motion can be treated within the theory of stochastic processes, through the model of random walks [38]. In this context, the probability distribution $P(\mathbf{r},t)$ of finding a water molecule at position $\mathbf{r}$ at time t can be defined in terms of a propagator $P(\mathbf{r},\mathbf{r}_o;t)$ which describes the evolution in space and time of the initial particle distribution $P(\mathbf{r}_o,0)$,

$$P(\mathbf{r},t)=\int_{-\infty}^{+\infty}P(\mathbf{r},\mathbf{r}_o;t)P(\mathbf{r}_o,0)d^3\mathbf{r}_o\,. \tag{1}$$

For an initial distribution given by the Dirac δ function, corresponding to a particle at the origin ($\mathbf{r}_o=0$) at $t=0$, the probability distribution $P(\mathbf{r},t)$ formally equals the propagator expression $P(\mathbf{r},\mathbf{r}_o;t)$ [38]. For Markovian processes, in which the random walker loses memory of previous jumps at each step, $P(\mathbf{r},t)$ obeys the general Fokker-Planck equation:

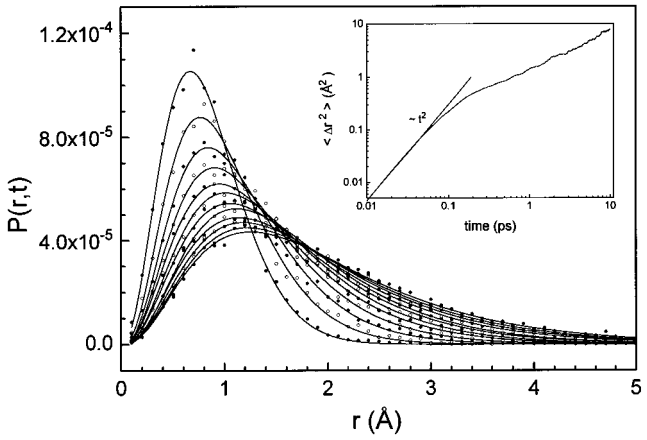

FIG. 1. Probability distribution $P(\mathbf{r},t)$ of water molecules walking within 4 Å from the protein surface, as a function of the traveled distance, for different times, from 0.5 ps (the highest curve) to 6 ps (the lowest curve) with a time step of 0.5 ps. Solid lines have been plotted as guides to the eye. Inset: log-log plot of the water oxygen mean square displacement, as a function of time, calculated for the same water ensemble; the free flight curve ($\sim t^2$) is also shown.

$$\frac{\partial P(\mathbf{r},t)}{\partial t}+\nabla[A(\mathbf{r})P(\mathbf{r},t)]=\tfrac{1}{2}\nabla^2[B(\mathbf{r})P(\mathbf{r},t)], \qquad (2)$$

where $A(\mathbf{r})$ and $B(\mathbf{r})$ are the first and the second moments of $P(\mathbf{r},t)$, respectively.

When the second term of the left hand side is zero, and $B(\mathbf{r})$ is a constant, Eq. (2) describes a particle diffusing freely with a diffusion coefficient D proportional to B. The solution of such an equation, which suitably represents many different diffusive processes [39], among which is self-diffusion of bulk water at room temperature, results in a Gaussian probability distribution which is generally written as

$$P(\mathbf{r},t)=\left(\frac{1}{4\pi Dt}\right)^{d/2} e^{-(d\mathbf{r}^2/2Dt)}, \qquad (3)$$

where d is the spatial dimension.

For fully hydrated PC, we evaluated $P(\mathbf{r},t)$ directly from the MD trajectories, by averaging over all the water molecules moving within a layer of 4 Å from the protein surface and covering a distance $|\mathbf{r}|$ during a flight time t. A collection of curves representing $P(\mathbf{r},t)$ at fixed, equally spaced, time values from 0.5 to 6 ps is shown in Fig. 1. In the analyzed temporal region, the mean square displacements (see inset) show, at long times, a linear trend, in the log-log plot; such a behavior points out that the diffusive regime was reached after about 0.2 ps. All the curves in Fig. 1 are characterized by a bell-shaped trend which largely deviates from a Gaussian, as it would instead be expected for Brownian diffusing particles. In addition, a peak shift of the $P(\mathbf{r},t)$ curves toward larger traveled distances is registered as far as longer times are taken into account.

The mean square displacement $\langle \Delta r^2 \rangle$ of diffusing water molecules is strictly related to the water molecule probability distribution by the relationship [40]

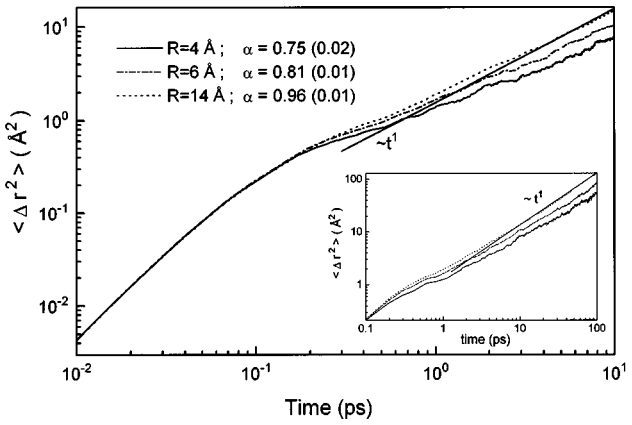

FIG. 2. Mean square displacements of water versus time for the fully hydrated plastocyanin system by restricting the analysis to water molecules moving within layers characterized by different distances from the protein surface. A layer of radius R is defined as the region including all the points whose minimum distance to any protein atom is less than or equal to R: $R=4$ Å (solid line), $R=6$ Å (dot-dashed line), and $R=14$ Å (dotted line). Each curve was obtained by averaging over 20 different time origins and over the corresponding water ensemble. The values of α reported in the figure were extracted by a fit of the curves, in the time interval from 1 to 10 ps, according to Eq. (6). Standard deviations are reported in parentheses. The heavy line indicates a trend of $\langle \Delta r^2 \rangle$ as $\sim t^1$. Inset: mean square displacements for the same water ensemble in the time interval 0.1–100 ps.

$$\langle \Delta r^2 \rangle = \int d^3\mathbf{r}\; r^2 P(\mathbf{r},t). \qquad (4)$$

Integrating Eq. (4) by using a Gaussian form for the propagator, the expected result within the Brownian kinetic theory is obtained:

$$\langle \Delta r^2 \rangle = 6Dt \qquad (5)$$

valid for t values after which the initial transient has decayed. Practically, this condition is fulfilled for times longer than the correlation time τ_{corr} of the velocity autocorrelation function (discussed later) [40].

On the other hand, the water oxygen mean square displacements versus t can be evaluated directly from the MD simulation data. Figure 2 shows the mean square displacements $\langle \Delta r^2 \rangle$ in a log-log plot, averaged over all the water molecules belonging to the three layers of different thickness ($R=4$, 6, and 14 Å) defined above, in a time interval Δt of 10 ps. At very short times (less than approximately 0.2 ps), before the diffusive regime is established, the behavior of $\langle \Delta r^2 \rangle$ for the different curves is almost indistinguishable. After the break, the $\langle \Delta r^2 \rangle$ trends appear linear with time but with different slopes in the log-log plot, all the curves displaying a slope smaller than that corresponding to normal diffusion ($\langle \Delta r^2 \rangle \sim t^1$ also shown in Fig. 2) [41]. In addition, the slopes progressively decrease for solvent layers approaching the protein surface. The same trend of $\langle \Delta r^2 \rangle$ is observed also for a longer (100 ps) time interval (see the inset of Fig. 2).

We fit the curves of Fig. 2, in the time interval from 1 to 10 ps, to a law:

$$\langle \Delta r^2 \rangle \sim t^{\alpha}. \tag{6}$$

The α values extracted from the fit are reported in Fig. 2; all the values found are smaller than 1. For water diffusing in the largest region ($R=14$ Å), α is found to be very close to 1 (0.96). In addition, the value of the diffusion coefficient ($D=0.26$ Å^2/ps), obtained from the limiting slope of the $\langle \Delta r^2 \rangle$ plot, is in agreement with that estimated for bulk SPC/E water [30]. As long as smaller distances from the protein surface are considered, the α exponent is found to decrease: $\alpha=0.81$ for the layer of thickness $R=6$ Å, and $\alpha=0.75$ for $R=4$ Å being obtained. These results show that anomalous diffusion takes place for water molecules moving in the proximity of the protein surface, while the anomaly is less pronounced when the contribution to $\langle \Delta r^2 \rangle$ of waters moving far from the surface is predominant [22]. Since values less than one are registered for α, dispersive diffusion, indicative of retarded motion with respect to the Brownian behavior, occurs for hydration water [28].

In the presence of anomalous diffusion, the slope of $\langle \Delta r^2 \rangle$ changes with time, and an evaluation of D by means of Eq. (5) could lead to both an incorrect and t-dependent value for D. This fact might be at the origin of the numerous discrepancies found in the water diffusion coefficient, especially when an analysis of D as a function of the distance from the protein is performed [2,24,42–44]. In this context, some caution has been suggested [22] in the use of the self-diffusion coefficient to characterize the water dynamics in the above mentioned systems. Alternatively, an effective diffusion coefficient D_{eff}, depending on distance traveled, can be introduced [45]:

$$D_{\mathrm{eff}} = \frac{d\langle \Delta r^2 \rangle}{dt} \simeq \langle \Delta r^2 \rangle^{(\alpha-1)/\alpha}. \tag{7}$$

Such an equation could provide a more reliable way to quantify, in the temporal window of interest, the water local mobility around a protein macromolecule.

The dynamical behavior of interfacial water can be described in a different way by evaluating the water molecule residence times in the first, or successive, hydration shells of protein atoms exposed to the solvent [18,20,21,46] from an appropriately defined ''survival-time-correlation function'' [21,47], describing the relaxation of the atomic hydration shells. This method, which proved to be extremely valuable in the local characterization of the PC-water interface [20,48], can also be employed to study the relaxation of the entire water layer around the protein body. In this context, the ''layer survival-time-correlation function'' can be defined as

$$C_R(t) = \frac{1}{N_W} \sum_{j=1}^{N_W} \frac{\langle p_{R,j}(0) p_{R,j}(t) \rangle}{\langle p_{R,j}(0)^2 \rangle} \tag{8}$$

in which $p_{R,j}(t)$ is a binary function that takes the value of *one* if the jth water molecule stays in the layer of thickness R, for a time t without getting out in the interim of this interval, and of *zero* otherwise. This quantity $C_R(t)$ measures the probability that a water molecule remains in a given layer at a certain time t, without having ever exchanged with bulk water before.

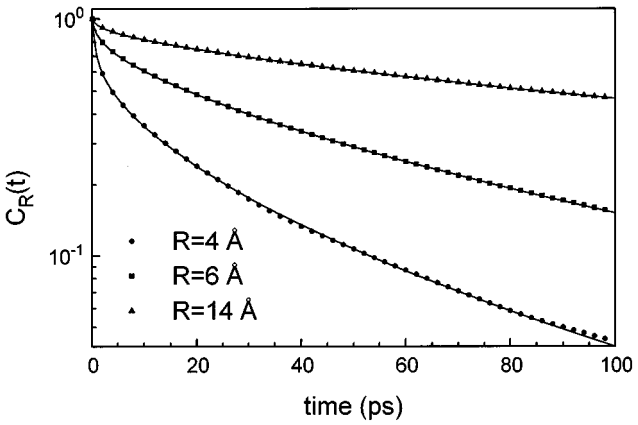

FIG. 3. Semilog plot of the survival-time-correlation function $C_R(t)$ for the three water layers considered: dots ($R=4$ Å), squares ($R=6$ Å), and up triangles ($R=14$ Å). The solid lines are the fitting curves obtained by Eq. (10). The parameters extracted by the fit are reported in Table I.

In Fig. 3, the function $C_R(t)$, evaluated from MD trajectories according to Eq. (8), is plotted versus t for the three water layers considered. All the three curves show the same trend which consists of a fast initial decay, on a time scale of picosecond or even less, followed by a slower decay. For the largest water layer ($R=14$ Å), involving a large portion of waters which move quite far from the protein surface, it can be observed that the long-time relaxation is almost linear in the semilog plot, indicating that the long-time decay of the survival-time-correlation function can be approximately well described by a single exponential relaxation. This result is consistent with relaxation properties observed in bulk water [41]. As far as water layers progressively closer to the protein surface are taken into account, a single exponential decay is no longer followed, as put into evidence by the significant deviation of the curves for $R=6$ and 4 Å from a straight line in the semilog plot. It turns out, instead, that in these cases, the long-time decay can be accurately described by a stretched exponential [Kohlrausch-Williams-Watts (KWW)] [49]:

$$C_R(t) \sim A e^{-(t/\tau)^{\beta}}, \tag{9}$$

which is largely employed in the characterization of the non-exponential nature of relaxations in several phenomena in complex condensed matter systems [50]. The KWW time constant τ provides the time scale over which the process evolves: in our case, it gives an estimate of the residence time of waters in the considered solvent layer. The exponent β is the signature of relaxation in disordered media [27,50]: the smaller is the value of β, the largest deviation of the relaxation functions from an exponential occurs; while, if $\beta=1$, the single exponential is recovered. However, Eq. (9) could not fit the entire relaxation trend shown in Fig. 3, as data concerning the fast initial decay are not well reproduced. A fast initial relaxation superimposed on the long, stretched one has already been observed in many different

TABLE I. Stretched exponential time constants (τ_s, τ_l) and exponents (β_s, β_l) extracted by a best fit, according to Eq. (10), of the survival-time-correlation function $C_R(t)$ of water hydration shell for different layers.

Layer	τ_s (ps)	β_s	τ_l (ps)	β_l
0–4 Å	0.37±0.03	0.79±0.05	13.4±0.2	0.54±0.03
0–6 Å	0.38±0.09	0.70±0.05	39.9±0.6	0.64±0.01
0–14 Å	1.25±0.05	0.60±0.04	164±2	0.69±0.02
10–14 Å	0.31±0.05	0.80±0.02	5.31±0.09	0.90±0.05
14–18 Å	0.59±0.05	0.67±0.01	7.5±0.1	0.97±0.03

relaxation processes [50], due to the presence of a transient phenomenon which usually decays on a very short-time scale compared to the relaxation itself; in some cases, the fast decay is modeled as a single exponential [50]. We found, instead, that also the short-time relaxation can be reliably described by a stretched exponential law. Thus a suitable formulation, able to reproduce both the short and the long-time decay of $C_R(t)$, is given by

$$C_R(t)=Ae^{-(t/\tau_s)^{\beta_s}}+Be^{-(t/\tau_l)^{\beta_l}}, \tag{10}$$

which is a sum of two stretched exponentials, characterized by different time constants: one for the short- (τ_s) and another one for the long- (τ_l) time decay, and also by different β values. A fitting procedure of data shown in Fig. 3, by Eq. (10), allowed us to successfully describe the $C_R(t)$ trends for all three water layers (see solid lines in Fig. 3); the extracted parameter values are reported in Table I. From this table, it can be noticed that the values of τ_s, relative to the fast dynamics, are found to be of the order of 1 ps or less, for all three water layers considered. Such a fast transient in $C_R(t)$ could be due to the fact that water molecules vibrate and liberate inside a microscopic cage formed by their nearest neighbors, before escaping from such structures. During such a motion, water molecules close to the border of a solvent layer might cross forward and backward across its surface, thus giving rise to the fast initial decay of the hydration layer relaxation function. This picture of water dynamical behavior near the protein surface is reminiscent of that introduced through the mode coupling theory for supercooled bulk water [51]. Also in that case, the formation of a cage of nearest neighbors, which at low temperatures persists over a longer-time scale, is able to explain the relaxation properties of water. In this respect, such a result provides a further support to the close analogy between water in the proximity of a protein surface and bulk water at low temperature. For what concerns the stretched exponent β_s, it can be seen that it is of the order of 0.7, slightly increasing from the largest to the thinnest water shell. The last two columns of Table I report τ_l and β_l, describing the long-time decay of $C_R(t)$. As expected, the relaxation times of hydration shells are very different according to which layer is considered: for the smallest one a τ_l of 13.4±0.2 ps is found in good qualitative agreement with residence times of water molecules in atomic shells of radius 4 Å around charged and polar atomic hydration sites [20]. This fact seems to indicate a dominance of charged sites in the regulation of the first layer water behavior. Residence times of water in the two largest shells, instead, appear to be quite high, being $\tau_l=39.9\pm0.6$ ps for the 0–6 Å layer and $\tau_l=164\pm2$ ps for the 0–14 Å one. These results are consistent with the fact that the larger the layer, the slower the exchange with bulk water. As previously mentioned, the exponent β_l of the stretched long relaxation is found to decrease for water layers in which the influence of superficial waters is progressively larger. However, the exponent β_l for the largest water layer still greatly differs from unity, being only $\beta_l=0.69$. This seems to be in disagreement with what is found for the mean square displacement analysis, from which water molecules in the largest shell recover features typical of bulk water. Evidently, even if a large portion of waters weakly affected by the protein is involved in the largest shell, molecules moving close to the protein surface (characterized by a high anomalous behavior) make a significant contribution to the layer relaxation process. To better investigate such an aspect, we evaluated the function $C_R(t)$ for two more solvent layers, both of thickness 4 Å and involving water molecules walking from 10 to 14 Å and from 14 to 18 Å. Because of the large distance from the surface, the influence of the protein on these water layers should be quite low. Actually, from the last two rows of Table I, it can be seen that the β_l exponent becomes very close to one. Furthermore, it should be noticed that τ_l values in the 10–14 and 14–18 Å shells are slightly lower than that observed in the 0–4 Å shell, indicating an enhanced mobility of waters far from the surface with respect to that occurring in the proximity of the protein surface. Finally, it should be noted that also for these two shells, the short-time decay shows essentially the same features observed for the previous shells.

B. Translational and reorientational motions

The study of the mean square displacements has shown that the diffusion of water molecules close to the protein surface has an anomalous character. In order to get further information on the solvent diffusional motion, both translational and rotational, we evaluated the water translational velocity autocorrelation function and the reorientational autocorrelation function. The former, which is defined as

$$C_{vv}=\frac{\langle \mathbf{v}(0)\cdot\mathbf{v}(t)\rangle}{\langle \mathbf{v}(0)^2\rangle}, \tag{11}$$

has been calculated from the water trajectories for the three layers of different thickness defined above, and has been plotted in Fig. 4. From this figure, it comes out that within 1 ps, all the C_{vv} curves have been practically decayed to zero. Since the translational motion assumes diffusional characteristics in times after which C_{vv} has decayed to zero, it comes out that for our system the diffusive regime is reached within 1 ps, such a behavior being also found for the first layer water molecules whose motion is partially slowed down by the presence of protein macromolecule. Thus the sublinear trend of the mean square displacements with time should not be attributed to a difficulty in reaching the diffusional regime, but essentially to a modified nature of the diffusive process itself [22].

All three C_{vv} curves in Fig. 4 after some time become negative because of the ''rebound'' of molecules from the

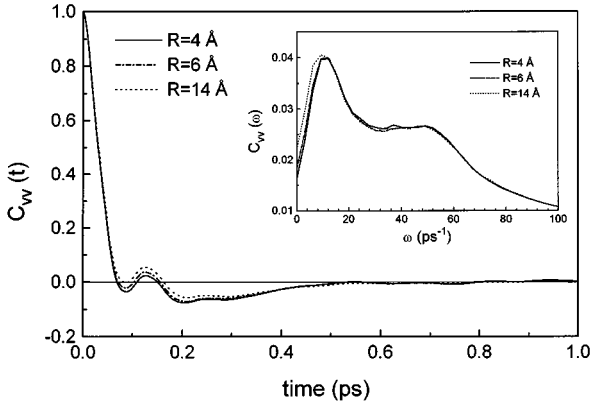

FIG. 4. Translational velocity autocorrelation function for water molecules belonging to the three progressively thicker layers defined in Fig. 2. Inset: power spectra of the velocity autocorrelation functions.

shell of their neighbors, and then they show a positive bump according to what is observed in bulk water [52]. This bump is shifted toward more negative values for waters confined in layers closer to the protein surface. Similar results are obtained for a different protein, ubiquitin [15], and for a hydrophobic solute in an aqueous environment [37]. Since the oscillations manifested in the velocity autocorrelation functions are generally due to many body intermolecular potentials, the differences among the C_{vv}, registered for the three different solvent layers, indicate that water molecules can be subjected to slightly different forces according to the region to which they belong. The Fourier transform of the C_{vv}, reported in the inset of Fig. 4, is characterized, for all the curves, by one peak at angular frequency of about $w(=2\pi\nu)=10$ ps^{-1} and by a shoulder at about $w=50$ ps^{-1}; such results are in good agreement with those observed in bulk water [52]. Since the diffusion process in liquids can be viewed as a succession of jumps after which a water molecule imprisoned by its neighbors behaves in a solidlike manner, the frequency distribution of the power spectrum can be interpreted as the density of states of independent oscillators. Then, a peak in the frequency spectrum represents the population of a mode of a given frequency, related to the vibration of water molecules. For water molecules moving within 6 Å (0–4 and 0–6 Å shells) from the protein surface, a slight shift of the main peak towards higher frequency is observed with respect to waters moving in the larger shell. This can be due to a tightening of the forces acting on the molecule, making it vibrate at a higher frequency in the microscopic cage formed by its nearest neighbors. Such vibration occurs on the time scale of fractions of 1 ps, and is in good agreement with the fast temporal scale dynamics displayed by the hydration shell relaxation.

The rotational diffusion of water has been analyzed through the reorientational dynamics of its electrical dipole $\boldsymbol{\mu}$ which is defined as the vector (molecule-fixed) pointing from the water oxygen to the middle point of the two hydrogen atoms. The time behavior of $\boldsymbol{\mu}$ has been determined by means of the autocorrelation functions Γ_l of the Legendre polynomials $P_l(\cos\theta)$. The functions Γ_l are defined as

$$\Gamma_l(t)=\langle P_l(\hat{\boldsymbol{\mu}}(0)\cdot\hat{\boldsymbol{\mu}}(t))\rangle, \tag{12}$$

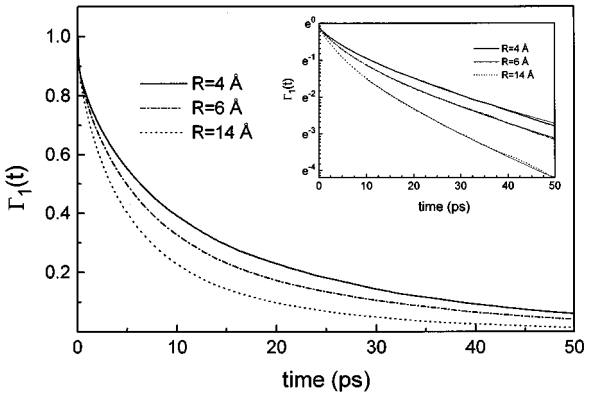

FIG. 5. Rotational reorientation of the water molecule dipole direction for $l=1$ [see Eq. (12)]. The curves, corresponding to the three different layers, are depicted as in Fig. 2. Inset: the same plot, but in a semilog scale. Continuous thin lines are the best-fit curves obtained by Eq. (9); the fitting parameters are reported in Table II.

where $\hat{\boldsymbol{\mu}}(t)$ is the unit vector along the molecular dipole axis at time t. The trends of Γ_1 and Γ_2 as a function of time are shown in Figs. 5 and 6, respectively. Both Γ_1 and Γ_2 decay toward zero with different rates according to the water layer considered. In each case, however, reorientation appears to be slower for water molecules belonging to the 0–4 Å solvent layer. This means that, on average, the reorientational diffusion turns out to be retarded for water molecules moving in the proximity of the protein surface, possibly due to stronger solvent-solute interactions with respect to those of water farther from the macromolecule. Interestingly enough, the long-time decay of the reorientational time-correlation function could not be described by a single exponential law, as can be seen in the insets of Figs. 5 and 6 (for Γ_1 and Γ_2, respectively), where a deviation from a straight line in the semilog plot is evident. According to what is found for the relaxation of the survival time correlation function, a KWW stretched exponential decay suitably describes the long term decay. Solid lines in the insets of Figs. 5 and 6 represent the best-fit curves according to Eq. (9); the corresponding values for τ and β are reported in Table II. For both Γ_1 and Γ_2, the

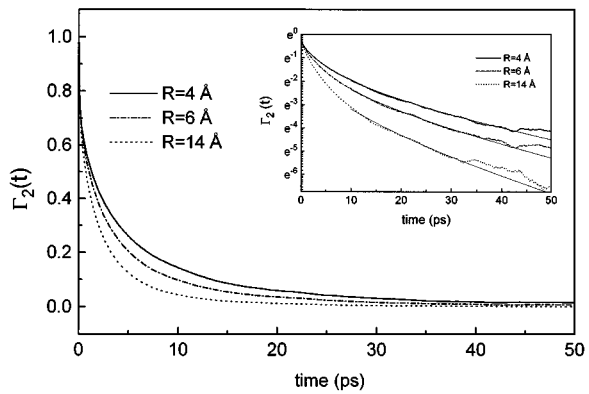

FIG. 6. Rotational reorientation of the water molecule dipole direction for $l=2$ [see Eq. (12)]. The curves, corresponding to the three different layers, are denoted as in Fig. 2. Inset: the same plot, but in a semilog scale. Continuous thin lines are the best-fit curves obtained by Eq. (9); the fitting parameters are reported in Table II.

TABLE II. Stretched exponential [Eq. (9)] fitting parameters τ and β of the reorientational autocorrelation functions Γ_1 and Γ_2, corresponding to long-time decay, of hydration water in different layers.

	Γ_1		Γ_2	
Layer	τ (ps)	β	τ (ps)	β
0–4 Å	9.7±0.2	0.63±0.04	4.80±0.05	0.59±0.03
0–6 Å	9.0±0.3	0.65±0.09	4.21±0.04	0.62±0.03
0–14 Å	7.4±0.2	0.72±0.06	3.50±0.02	0.66±0.04

time constants of the stretched exponentials are progressively larger as far as waters closer to the protein surface are taken into account; such a behavior gives a quantitative estimate of the retardation effect exerted by the protein on superficial water reorientation. In comparison to Γ_1, however, the relaxation of Γ_2 occurs on a significantly faster time scale. Moreover, the β exponent values show that the deviation from the single exponential decay is more marked for water molecules belonging to the layer closer to the surface. The previous analysis, regarding both translational and rotational diffusion of water, shows, on average, a retardation in the motion of solvent molecules near the protein surface, with respect to that of bulk water. Similar results have been obtained for water around a hydrophobic solute [37] and also around a different protein, ubiquitin [15]. Generally, both the sublinear trend of the mean square displacements and the stretched exponential form of Γ_1 and Γ_2 relaxations point out that the very nature of the diffusive process (both translational and rotational) is deeply affected by the presence of a biological macromolecule.

IV. DISCUSSION

Different dynamical properties of water at 300 K, perturbed by a biological solute, have been analyzed. Generally, our results point out that the presence of the protein deeply influences the dynamics of water molecules, especially in proximity to the protein surface even if some effects are also found at rather large distances from the macromolecule. The Brownian motion, which generally represents a suitable model for the description of self-diffusion of bulk water at room temperature [39], is no longer able to describe the solvent diffusive process in the protein-solvent interfacial region. In addition, the relaxation of the survival time-correlation functions, as well as of the reorientational functions, significantly deviates from an exponential behavior, such functions being instead satisfactorily described by a stretched exponential law. This behavior indicates that the dynamical features of hydration water cannot be explained by the stochastic master equations which are usually employed to describe Markovian processes. Generally, to characterize a random walk, two functions are to be defined [38]: the first is the distribution of the step lengths that generate the walk, and the second is the distribution of waiting times between steps. The finiteness of the first two moments of the step distribution function and of the first moment of the waiting time distribution [38] are required to derive the Fokker-Planck master equation for a random walk; certain interesting examples of stochastic processes violating the finite moment requirement have been observed. Lévy [53] and subsequently Mandelbrot [54] have investigated the case of no finite second moment in the step length, a situation which yields the common observed asymptotic inverse power law distribution for the total displacement of the walkers. Scher and Montroll [55] and Shlesinger [56] have studied instead the case of no finite moments in the waiting time distribution. In this context, deviations from Brownian particle diffusion can be attributed to random walks in geometrically disordered fractal structures and/or to temporal disorder, both having underlying scale-invariant properties, spatial or temporal, with no characteristic length or time scales [55,57]. The anomalous features displayed by the protein-solvent system, and indicating a strong deviation from Markovian random walk processes, should be traced back to the topological and dynamical disorder peculiar to these systems. For example, it has been shown that solvent accessible surfaces of different globular proteins, among which is PC, are characterized by roughness and some kind of self-similarity, which is reminiscent of that of a fractal surface [58,59]. Indeed, protein surfaces have been modeled as fractal surfaces with dimension greater than 2 [58,59]. In particular, for PC, a fractal dimension $\overline{d}=2.18$ was calculated from the x-ray structure [59].

The exploration of the rough surface from the water molecules moving in the vicinity of the macromolecule could affect the solvent diffusive behavior. Actually, the dispersive transport regime, which we have found to characterize water molecule motion around PC, is consistent with the model describing random walks on fractal structures [28,60,61]. In these models, in fact, as a consequence of the scaling properties of the fractal structure, the mean square displacement can be expressed by

$$\langle \Delta r^2 \rangle \sim t^{\tilde{d}/\overline{d}}, \tag{13}$$

where $\overline{d}$ is the fractal dimension of the surface and $\tilde{d}$ is its spectral dimensionality, the last being a quantity related to the connectivity of the protein tertiary structure [62]. If the long term mean square displacements, shown in Fig. 2, are fitted by Eq. (13), using a value of 2.18 for fractal dimensionality, the following values for the spectral dimensionality can be extracted: $\tilde{d}=1.64$ for the 0–4 Å layer, and $\tilde{d}=1.77$ and 2.09 for the other two layers, respectively. These results point out that the spectral dimensionality of the protein structure appears to be different if waters close to the protein surface or water molecules traveling quite far from it are taken into account. In the presence of surface roughness, an expression for the water molecule probability distribution has been derived [28]. It consists in a non-Gaussian propagator given by [25,28,62]

$$P(\mathbf{r},t)=t^{-\tilde{d}/2} f(\xi), \tag{14}$$

which involves a function $f(\xi)$ of a scaling variable ($\xi = r t^{-\tilde{d}/2\overline{d}}$) expressed by

$$f(\xi) \sim \exp(-a_0 \xi^{2\overline{d}/\tilde{d}}) \quad \text{for } \xi<1, \tag{15}$$

$$f(\xi) \sim \xi^{\beta} \exp(-a_1 \xi^{\nu}) \quad \text{for } \xi>1, \tag{16}$$

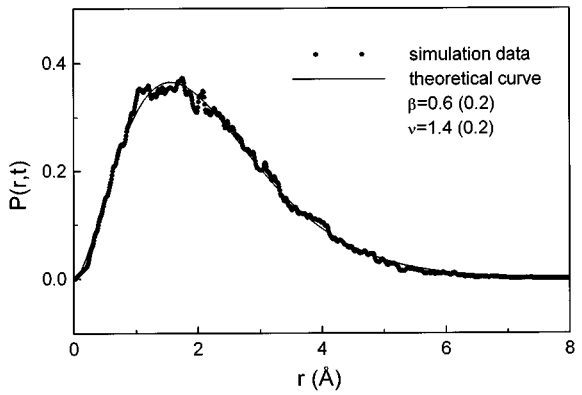

FIG. 7. Probability distribution $P(\mathbf{r},t)$ as a function of the traveled distance r for $t=5$ ps, calculated from the MD trajectories of waters moving within 4 Å from the protein surface. The continuous line is the best-fit curve as obtained by using Eq. (14). The fitting parameters are also shown (standard deviations are reported in parentheses).

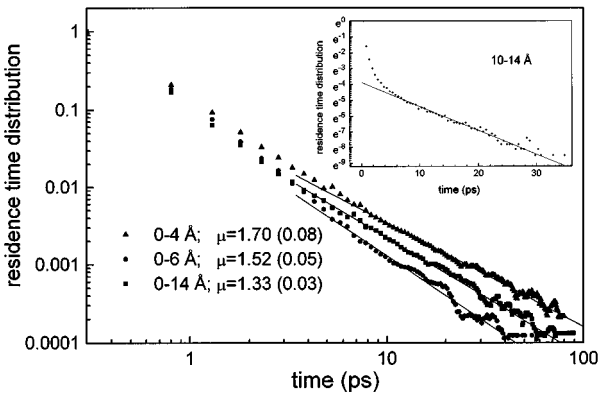

FIG. 8. Log-log plot of the residence time distribution, as a function of the time interval t, for solvent molecules residing in layers of different thickness. Continuous lines are the best-fit curves obtained by Eq. (18). The fitting parameters are also shown (standard deviations are reported in parentheses). Inset: the semilog plot of the same distribution for the water layer 10–14 Å. The continuous line is the best-fit curve obtained by Eq. (19).

β and ν being

$$\beta=\frac{\overline{d}(\widetilde{d}-1)}{2\overline{d}-\widetilde{d}}, \quad \nu=\frac{2\overline{d}}{2\overline{d}-\widetilde{d}}. \tag{17}$$

When $\overline{d}=\widetilde{d}=2$, as it is for the standard diffusion on a regular medium, the Gaussian shape of the propagator is recovered. Instead for $\overline{d}\neq\widetilde{d}\neq 2$, the expression in Eq. (14) manifests strong deviations from the Gaussian behavior, being an ''enhanced Gaussian'' for small values of the scaling variable ξ, or a ''stretched Gaussian'' for large ξ. We tried to fit $P(\mathbf{r},t)$, calculated from the MD trajectories, by means of Eq. (14); a good agreement between the theoretical and the MD simulated $P(\mathbf{r},t)$ was obtained. The result of the fit for $\xi>1$ is shown in Fig. 7 for a selected time value; the extracted parameters β and ν are also reported. These values are found to be quite close to those directly calculated through Eq. (17), by introducing the corresponding d value for PC [59] and the $\widetilde{d}$ value previously determined from the mean square displacement curves ($\beta=0.50\pm0.01$ and $\nu=1.60\pm0.01$). The evidence that the functional form of the propagator [Eq. (14)] reproduces so well the computed data supports the hypothesis that the protein surface roughness, modeled as a fractal surface, could really affect the water dynamical behavior and then could be at the origin of the evidenced anomalous diffusional behavior.

On the other hand, the anomalies in the water diffusive process might also be ascribed to a temporal disorder in the dynamical behavior [27,38,63]. Water molecule diffusion over the protein surface is deeply affected by both the protein structure and dynamics. In fact, water molecules walking in the vicinity of the protein could interact, also by forming HB, with superficial protein atoms; such interaction, strongly dependent on the electrostatic as well as on the polar character of the amino acid residues, reveals a large variability from site to site [19,20]. In addition, the continuous protein motion, including the CS transitions and involving a wide range of time scales, can modulate the landscape over which water molecules are moving, producing traps or local forces to which solvent molecules are submitted [64]. This picture suggests that the variety of chemicophysical properties of the amino acid residues exposed to the solvent, together with the protein motions, are able to modulate the times that water molecules spend at the various protein hydration sites. In this connection, it should be remarked that a spread in the residence times was registered by both NMR and MD investigations [18,20] for water molecules around different protein macromolecules. In particular, the residence time distribution of waters within 4 Å from the PC surface, extracted by computing the number of MD steps that a water molecule resides in a given layer during a time interval t, is shown in Fig. 8 in a log-log plot. Such an approach, similar to that used in previous works [20,25], allowed us to directly measure residence times in the whole solvent layer around the protein. For all the analyzed solvent layers involving, at least partially, molecules closer to the protein surface, the distribution for residence times shows long tails which are very well described by an inverse power law:

$$\psi(t)\sim t^{-\mu}. \tag{18}$$

The exponents μ, extracted as the slope of straight lines in a log-log plot, are reported in Fig. 8. In particular, the value of $\mu=1.70\pm0.08$ for the 0–4 Å layer, is in satisfactory agreement with that ($\mu=1.5\pm0.2$) found for the local atomic distribution of residence times [20,25], by using a different approach. The presence of such a distribution for residence times of water molecules leads to the interpretation of their motion as a series of steps which do not occur only at fixed time intervals, but are regulated by a waiting time distribution $\psi(t)$ given by Eq. (18). On the contrary, for Brownian motion, the probability of remaining at a given site during the time interval t decays exponentially in time [27]:

$$\psi(t)\sim e^{-(bt)}. \tag{19}$$

Such a trend is registered when the solvent layer 10–14 Å, which involves solvent molecules with predominant bulk water features, is taken into account. Actually, as can be

inferred from the inset of Fig. 8, the long tail in the semilog plot reveals a linear trend with time as predicted by Eq. (19). In the presence of a distribution of waiting times characterized by an inverse power law, with an exponent μ smaller than 2, such as that obtained for PC hydration water, a nonlinear temporal dependence for the mean square displacements can be derived [28,65,66]:

$$\langle \Delta r^2 \rangle \sim t^{\mu-1}. \tag{20}$$

Actually, Eq. (20) could provide a way of calculating μ from the long-time mean square displacement trend. The value of μ ($\mu = 1.75 \pm 0.05$) extracted according to such a procedure for the 0–4 Å layer, turns out to be slightly higher than that previously obtained (see Fig. 2), the two values being consistent.

As in the case of diffusion on a fractal surface, the sublinear trend of $\langle \Delta r^2 \rangle$ can be ascribed to a non-Gaussian propagator, which can be modeled as [28]

$$P(\mathbf{r},t) = t^{-(\mu-1)/2} f(\xi), \tag{21}$$

where $\xi = r t^{-(\mu-1)/2}$ and $f(\xi)$ is

$$f(\xi) \sim \exp^{-a_1 \xi - a_2 \xi^2} \quad \text{for } \xi < 1, \tag{22}$$

$$f(\xi) \sim \xi^{\beta} \exp^{-b_1 \xi^{\nu}} \quad \text{for } \xi > 1, \tag{23}$$

where β and ν in this case are given by means of μ:

$$\beta = \frac{2-\mu}{3-\mu}, \quad \nu = \frac{2}{3-\mu}. \tag{24}$$

It is evident that a deviation of Eq. (21) from a Gaussian propagator occurs for $\mu \neq 2$. A good agreement between the theoretical curve, derived from Eq. (21) for $\xi > 1$, and the propagator data extracted from the MD trajectories is registered (results not shown). The corresponding values extracted from the best-fit procedure for β and ν ($\beta = 0.6 \pm 0.2$ and $\nu = 1.3 \pm 0.2$) are the same as those obtained by fitting the probability distribution of Fig. 7 with the stretched exponential propagator related to the fractal model [Eq. (14) coupled to Eq. (16)]. Such a result should not be surprising since the fitting expressions are formally equivalent, for fixed t, in the two cases. The β and ν values, as derived from the water probability distribution, can be compared with those calculated from Eq. (24), where for μ the value obtained from the water residence time distribution is introduced, i.e., $\beta = 0.2 \pm 0.1$ and $\nu = 1.5 \pm 0.2$. While the ν value is consistent with that arising from the fit of the probability distribution, the β value appears significatively lower.

Both models of a random walker in the presence of temporal and spatial disorder give a good description of water molecules motions in the region close to the protein surface; the stretched forms of the propagator can successfully describe the sublinear trend of the mean square displacements with time.

In order to complete this picture, it can be shown that also the stretched exponential decay of the hydration shell closer to the macromolecule is consistent with a non-Gaussian form for the propagator. In fact, an alternative method to evaluate the hydration layer relaxation function $C_R(t)$ can be derived

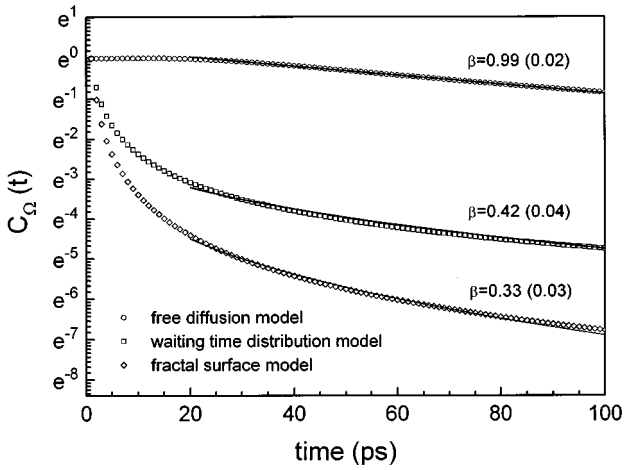

FIG. 9. Semilog plot of $C_\Omega(t)$ [Eq. (25)] evaluated for the spatial region corresponding to a sphere of radius $R = 4$ Å, and for different expressions of the propagator according to the different models employed. Circles: Gaussian propagator [Eq. (3)]; squares: propagator predicted by the fractal model [Eq. (14)]; diamonds: propagator predicted by the continuous time random walk model [Eq. (21)]. Continuous lines are the best-fit curve obtained by Eq. (9); the extracted exponents β are also shown (standard deviations are reported in parentheses).

by the probability that, after a time t, a particle being in a spatial region Ω has survived without having ever escaped [67]:

$$C_\Omega(t) = \int_\Omega d^3\mathbf{r}\, P(\mathbf{r},t), \tag{25}$$

where the integral extends over the volume Ω. For Ω defined as a sphere of radius R (approximately describing the thickness of a water layer), Eq. (25) represents the probability that a water molecule has traveled less than R during a time interval t. In this particular case, the definitions given by Eqs. (8) and (25) conceptually coincide. In this context, we numerically evaluated the function $C_\Omega(t)$ using different expressions for the probability distribution: free diffusion, diffusion on a disordered structure, and diffusion governed by a distribution of waiting times. To represent the case of free diffusion on a regular medium, well described by the Brownian model, the Gaussian expression for $P(\mathbf{r},t)$ given in Eq. (3), and including, for the diffusion coefficient, the value $D = 0.26$ Å^2/ps extracted from the largest water layer, was used. Instead, for anomalous diffusion, the stretched exponential propagators [see Eqs. (14) and (21)], which describe the diffusive behavior on disordered (spatial or temporal) media well, have been employed, the values of the parameters obtained by the best-fit procedures having been introduced. The integral in Eq. (25) has been performed over a spatial region Ω corresponding to a sphere of radius $R = 4$ Å. The results of the integration are shown in Fig. 9. In the case of free diffusion, a single exponential relaxation has been obtained: such a result is consistent with the dynamics of a Brownian particle, whose probability of staying in a given spatial region, without having ever exchanged with bulk, decays according to a single exponential law. The other

two curves of Fig. 9, obtained by performing the integration exactly in the same conditions as in the first case, show a stretched exponential trend with β values reported in the plot. These values are in satisfactory agreement with those extracted from the long-time decay of the relaxation of the shell of thickness $R=4$ Å, the better agreement occurring when the temporal disorder model is taken into account. These results indicate that all the observed anomalies in the hydration water properties can be globally described in terms of a non-Gaussian propagator. In addition, they suggest that a closer description of the solvent propagator can be reached if disorder on a temporal scale is taken into account.

V. CONCLUSIONS

The presence of a biological solute in a water ensemble exerts a strong influence on the structural and the dynamical organization of the solvent. The very nature of the diffusive process (both translational and reorientational) of hydration water reveals drastic changes with respect to bulk water. In fact, not only is the mobility of water close to the protein surface on average hindered, but the appearance, in the log-log plot, of a sublinear trend with time for the mean square displacements reflects the occurrence of anomalous diffusion. In addition, the stretched exponential decay of the long-time tail for the reorientational time-correlation functions as well as for the relaxations for hydration water points out a complex dynamical behavior, very similar to that observed in other disordered systems.

All these features have been ascribed to a non-Gaussian form for the probability distribution of finding a particle somewhere in space and time. Such a behavior can be traced back to a spatial, as well as to a temporal, disorder of the protein-solvent system, also in connection with the amorphous character of hydration water.

[1] *Protein-Solvent Interactions*, edited by R. B. Gregory (Dekker, New York, 1995).

[2] V. Lounnas, B. M. Pettitt, and G. N. Phillips, Jr., Biophys. J. **66**, 601 (1994).

[3] W. Doster, A. Bachleitner, R. Dunau, M. Hiebl, and E. Lüscher, Biophys. J. **50**, 213 (1986).

[4] P. L. Poole and J. L. Finney, Biopolymers **22**, 255 (1983).

[5] H. Frauenfelder, F. Parak, and R. D. Young, Annu. Rev. Biophys. Biophys. Chem. **17**, 451 (1988).

[6] R. Elber and M. Karplus, Science **235**, 318 (1987).

[7] R. D. Young, H. Frauenfelder, J. B. Johnson, D. C. Lamb, G. U. Nienhaus, R. Philipp, and R. Scholl, Chem. Phys. **158**, 315 (1991).

[8] A. Ansari, J. Berendzen, S. F. Bowne, H. Frauenfelder, I. E. T. Iben, T. B. Sauke, E. Shyamsunder, and R. D. Young, Proc. Natl. Acad. Sci. USA **82**, 5000 (1985).

[9] J. L. Green, J. Fan, and C. A. Angell, J. Phys. Chem. **98**, 13 780 (1994).

[10] I. D. Kuntz and W. Kauzmann, Adv. Protein Chem. **28**, 239 (1974).

[11] J. L. Rupley, E. Gratton, and G. Careri, Trends Biochem. Sci. **8**, 18 (1983).

[12] P. J. Steinbach and B. R. Brooks, Proc. Natl. Acad. Sci. USA **93**, 55 (1996).

[13] I. E. T. Iben, D. Braunstein, W. Doster, H. Frauenfelder, M. K. Hong, J. B. Johnson, S. Luck, P. Ormos, A. Schulte, P. J. Steinbach, A. H. Xie, and R. D. Young, Phys. Rev. Lett. **62**, 1916 (1989).

[14] C. A. Angell, Science **267**, 1924 (1995).

[15] R. Abseher, H. Schreiber, and O. Steinhauser, Proteins: Struct. Funct. Genet. **25**, 366 (1996).

[16] C. L. Brooks III and M. Karplus, J. Mol. Biol. **208**, 159 (1989).

[17] G. Sartor and E. Mayer, Biophys. J. **67**, 1724 (1994).

[18] R. M. Brunne, E. Liepinsh, G. Otting, K. Wüthrich, and W. F. van Gunsteren, J. Mol. Biol. **231**, 1040 (1993).

[19] A. R. Bizzarri, C. X. Wang, W. Z. Chen, and S. Cannistraro, Chem. Phys. **201**, 463 (1995).

[20] C. Rocchi, A. R. Bizzarri, and S. Cannistraro, Chem. Phys. **214**, 261 (1997).

[21] A. E. Garcia and L. Stiller, J. Comput. Chem. **14**, 1396 (1993).

[22] A. R. Bizzarri and S. Cannistraro, Phys. Rev. E **53**, 3040 (1996).

[23] A. R. Bizzarri and S. Cannistraro, Europhys. Lett. **37**, 201 (1997).

[24] M. Levitt and R. Sharon, Proc. Natl. Acad. Sci. USA **85**, 7557 (1988).

[25] A. R. Bizzarri, C. Rocchi, and S. Cannistraro, Chem. Phys. Lett. **263**, 559 (1996).

[26] M. Settles and W. Doster, Faraday Discuss. R. Soc. of Chem. **103**, 269 (1996).

[27] A. Blumen, J. Klafter, and G. Zumofen, in *Transport and Relaxation in Random Materials*, edited by J. Klafter, R. J. Rubin, and M. F. Shlesinger (World Scientific, Singapore, 1985).

[28] J. Klafter, G. Zumofen, and A. Blumen, Chem. Phys. **177**, 821 (1993).

[29] W. F. van Gusteren and H. J. C. Berendsen, *Groningen Molecular Simulation (GROMOS) Library Manual* (Biomos, Groningen, 1987).

[30] H. J. C. Berendsen, J. R. Grigera, and T. P. Straatsma, J. Phys. Chem. **91**, 6269 (1987).

[31] J. M. Guss, H. D. Bartunik, and H. C. Freman, Acta Crystallogr., Sect. B: Struct. Sci. **48**, 790 (1992).

[32] A. G. Sykes, Adv. Inorg. Chem. **36**, 377 (1991).

[33] M. R. Redinbo, T. O. Yeates, and S. Merchant, J. Bioenerg. Biomembr. **26**, 49 (1994).

[34] H. J. C. Berendsen, J. P. M. Postma, W. F. van Gusteren, A. Di Nola, and J. R. Haak, J. Chem. Phys. **81**, 3684 (1984).

[35] J. P. Rickaert, G. Ciccotti, and H. J. C. Berendsen, J. Comput. Phys. **23**, 327 (1977).

[36] C. X. Wang, A. R. Bizzarri, Y. W. Xu, and S. Cannistraro, Chem. Phys. **183**, 155 (1994).

[37] D. A. Zichi and P. J. Rossky, J. Chem. Phys. **84**, 2814 (1986).

[38] E. W. Montroll and B. J. West, in *Fluctuation Phenomena*, edited by E. Montroll and J. L. Lebowitz, Studies in Statistical Mechanics Vol. VII (North-Holland, Amsterdam, 1987).

[39] J. W. Haus and K. W. Kehr, Phys. Rep. **150**, 263 (1987).

[40] D. Chandler, *Introduction to Modern Statistical Mechanics* (Oxford University Press, Oxford, 1987).
[41] J. P. Bouchaud and A. Georges, Phys. Rep. **195**, 127 (1990).
[42] P. Ahlström, O. Teleman, and B. Jönsson, J. Am. Chem. Soc. **110**, 4198 (1988).
[43] D. S. Hartsough and K. M. Merz, Jr., J. Am. Chem. Soc. **115**, 6529 (1993).
[44] M. Norin, F. Haeffner, K. Hult, and O. Edholm, Biophys. J. **67**, 548 (1994).
[45] G. Jug, Chem. Phys. Lett. **131**, 94 (1986).
[46] F. Brugè, E. Parisi, and S. L. Fornili, Chem. Phys. Lett. **250**, 443 (1996).
[47] R. W. Impey, P. A. Madden, and I. R. McDonald, J. Phys. Chem. **87**, 5071 (1983).
[48] C. Rocchi, Nuovo Cimento (to be published).
[49] R. Kohlrausch, Ann. Phys. (Leipzig) **12**, 353 (1847); G. Williams and D. C. Watts, Trans. Faraday Soc. **66**, 80 (1870).
[50] J. C. Phillips, Rep. Prog. Phys. **59**, 1133 (1996).
[51] P. Gallo, F. Sciortino, P. Tartaglia, and S. H. Chen, Phys. Rev. Lett. **76**, 2730 (1996).
[52] U. Balucani, J. P. Brodholt, and R. Vallauri, J. Phys.: Condens. Matter **8**, 6145 (1996).
[53] P. Lévy, *Calcul des Probabilities* (Gauthier-Villars, Paris, 1925).
[54] B. B. Mandelbrot, *The Fractal Geometry of Nature* (Freeman, San Francisco, 1982).
[55] H. Scher and E. W. Montroll, Phys. Rev. B **12**, 2455 (1975).
[56] M. F. Shlesinger, Annu. Rev. Phys. Chem. **39**, 269 (1988).
[57] G. Zumofen and J. Klafter, Phys. Rev. E **47**, 851 (1993).
[58] P. Pfeifer, U. Welz, and H. Wippermann, Chem. Phys. Lett. **113**, 535 (1985).
[59] C. D. Zachmann, S. M. Kast, A. Sariban, and J. Brickmann, J. Comput. Chem. **14**, 1290 (1993).
[60] J. Klafter, G. Zumofen, and A. Blumen, J. Phys. A **124**, 991 (1991).
[61] S. Havlin and D. Ben Havraham, Adv. Phys. **36**, 695 (1987).
[62] S. Alexander and R. Orbach, J. Phys. (France) Lett. **43**, 625 (1982).
[63] R. Bettin, R. Mannella, B. J. West, and P. Grigolini, Phys. Rev. E **51**, 212 (1995).
[64] F. H. Stillinger, Science **267**, 1935 (1995).
[65] M. F. Shlesinger, J. Stat. Phys. **10**, 421 (1974).
[66] J. Klafter, A. Blumen, and M. F. Shlesinger, Phys. Rev. A **35**, 3081 (1987).
[67] A. Szabo, K. Schulten, and Z. Schulten, J. Chem. Phys. **72**, 4350 (1980).